AMERICAN SOCIETY FOR MICROBIOLOGY | Journal of Bacteriology®

RESEARCH ARTICLE

NsrA, a Predicted β-Barrel Outer Membrane Protein Involved in Plant Signal Perception and the Control of Secondary Infection in *Sinorhizobium meliloti*

Anne-Marie Garnerone,[a] Fernando Sorroche,[a]* Lan Zou,[a] Céline Mathieu-Demazière,[a]* Chang Fu Tian,[a,b] Catherine Masson-Boivin,[a] Jacques Batut[a]

[a]Laboratory of Plant-Microbe Interactions, Université de Toulouse, INRA, CNRS, Castanet-Tolosan, France
[b]State Key Laboratory of Agrobiotechnology, College of Biological Sciences, China Agricultural University, Beijing, China

ABSTRACT An ongoing signal exchange fine-tunes the symbiotic interactions between rhizobia and legumes, ensuring the establishment and maintenance of mutualism. In a recently identified regulatory loop, endosymbiotic *Sinorhizobium meliloti* exerts negative feedback on root infection in response to unknown plant cues. Upon signal perception, three bacterial adenylate cyclases (ACs) of the inner membrane, namely, CyaD1, CyaD2, and CyaK, synthesize the second messenger cAMP, which, together with the cAMP-dependent Clr transcriptional activator, activates the expression of genes involved in root infection control. The pathway that links signal perception at the surface of the cell to cytoplasmic cAMP production by ACs was thus far unknown. Here we first show that CyaK is the cognate AC for the plant signal, called signal 1, that was observed previously in mature nodule and shoot extracts. We also show that inactivation of the gene immediately upstream of *cyaK*, *nsrA* (*smb20775*), which encodes a β-barrel protein of the outer membrane, abolished signal 1 perception *ex planta*, whereas *nsrA* overexpression increased signal 1 responsiveness. Inactivation of the *nsrA* gene abolished all Clr-dependent gene expression in nodules and led to a marked hyperinfection phenotype on plants, similar to that of a *cyaD1 cyaD2 cyaK* triple mutant. We suggest that the NsrA protein acts as the (co)receptor for two signal molecules, signal 1 and a hypothetical signal 1′, in mature and young nodules that cooperate in controlling secondary infection in *S. meliloti-Medicago* symbiosis. The predicted topology and domain composition of the NsrA protein hint at a mechanism of transmembrane signaling.

IMPORTANCE Symbiotic interactions, especially mutualistic ones, rely on a continuous signal exchange between the symbionts. Here we report advances regarding a recently discovered signal transduction pathway that fine-tunes the symbiotic interaction between *S. meliloti* and its *Medicago* host plant. We have identified an outer membrane protein of *S. meliloti*, called NsrA, that transduces *Medicago* plant signals to adenylate cyclases in the inner membrane, thereby triggering a cAMP signaling cascade that controls infection. Besides their relevance for the rhizobium-legume symbiosis, these findings shed light on the mechanisms of signal perception and transduction by adenylate cyclases and transmembrane signaling in bacteria.

KEYWORDS rhizobium, symbiosis, infection, adenylate cyclase, cAMP, transmembrane, *Medicago*, signaling, CHASE2

Rhizobia are alpha- and betaproteobacteria that achieve a symbiotic relationship with plant legumes (1, 2). Rhizobia thriving in the soil and the rhizosphere of plants sometimes elicit, on the roots of host legumes, the formation of specific organs, the nodules, which they colonize intracellularly and in which they fix atmospheric nitrogen,

Received 11 January 2018 **Accepted** 3 March 2018

Accepted manuscript posted online 12 March 2018

Citation Garnerone A-M, Sorroche F, Zou L, Mathieu-Demazière C, Tian CF, Masson-Boivin C, Batut J. 2018. NsrA, a predicted β-barrel outer membrane protein involved in plant signal perception and the control of secondary infection in *Sinorhizobium meliloti*. J Bacteriol 200:e00019-18. https://doi.org/10.1128/JB.00019-18.

Editor Anke Becker, Philipps-Universität Marburg

Address correspondence to Jacques Batut, jacques.batut@inra.fr.

* Present address: Fernando Sorroche, Laboratoire de Microbiologie et Génétique Moléculaires, Centre de Biologie Intégrative, Université de Toulouse, CNRS, UPS, Toulouse, France; Céline Mathieu-Demazière, Laboratoire de Microbiologie et Génétique Moléculaires, Centre de Biologie Intégrative, Université de Toulouse, CNRS, UPS, Toulouse, France.

A.-M.G. and F.S. are co-first authors.

to the benefit of the plant (3). The establishment of mutualism requires a sophisticated signal exchange between rhizobia and legumes (4). Early genome sequencing of *Sinorhizobium meliloti*, the *Medicago* symbiont, revealed a peculiar abundance ($n = 26$) of adenylate cyclases (ACs)/guanylate cyclases (GCs), suggesting that the secondary messengers cAMP and cGMP may play a prominent role in the environmental adaptation of these bacteria, including adaptation to symbiosis (5). ACs/GCs can be either cytoplasmic or attached to the inner membrane (6). The latter category includes three structurally similar ACs, i.e., CyaD1 (SMc02176), CyaD2 (SMc04307), and CyaK (SMb20776), consisting of a CHASE2 periplasmic domain (7) of unknown function and a cytoplasmic AC domain. These three ACs collectively contribute symbiotic adaptation in response to unknown plant signals (8). The CHASE2 domain was subsequently found to have a regulatory function, inhibiting AC activity in the absence of signal (8).

S. meliloti infects root hair cells via specialized structures called infection threads (ITs), which form in the epidermis (epidermal ITs [eITs]) before invading the root cortex (cortical ITs [cITs]) (9, 10). Early evidence indicated that IT formation is regulated along the nodulation process (11), but the underlying mechanisms remain unclear. Recently, we reported that eIT formation was (partially) unleashed upon inoculation of a *S. meliloti cyaD1 cyaD2 cyaK* triple mutant. In contrast to the wild type, the triple mutant elicits sustained eIT formation once nodules are formed; we called this process secondary infection, to distinguish it from primary eIT formation concomitant to nodulation. We have suggested that this feedback control of eIT formation results from modification of the root susceptibility to infection by endosymbiotic wild-type bacteria (8). Upon activation in nodules, the three ACs produce cAMP, which binds the Crp-like transcriptional activator protein Clr, which in turn activates a number of transcriptional targets directly and indirectly (12, 13). A few Clr targets of unknown biochemical function have been characterized to date, including *smc02178* and *smb20495*, whose mutants displayed on plants a hyperinfection phenotype similar to that of the *cyaD1 cyaD2 cyaK* triple mutant or a *clr* mutant (8, 12).

CyaD1, CyaD2, and CyaK activation takes place in response to unknown plant signals. Direct experimental evidence for one signal was obtained in nodule extracts of both infected and uninfected mature (14-day-postinoculation [dpi]) nodules (8), as well as in shoot extracts from both legumes and nonlegumes. Conversely, no conspicuous signal activity was detected in roots or young (7-dpi) nodules. However, the pattern of expression of a reporter *smc02178-lacZ* fusion in nodules indicated that *cyaK* and *cyaD1* (or *cyaD2*) had overlapping and complementary functions. Based on *in situ smc02178* gene expression patterns, CyaK was active in both young (7-dpi) and mature (14-dpi) nodules, whereas CyaD1 and CyaD2 activity was detected only in 7-dpi nodules (8). However, it was not known which of the three ACs sensed the signal observed in mature nodule and shoot extracts.

Here we first show that CyaK is the cognate AC for the signal evident in both mature nodule and shoot extracts. This signal was called signal 1. We then characterize a gene called *nsrA* (nodule signal receptor A), which is needed for both perception of signal 1 by CyaK and perception of a hypothetical signal 1′ by CyaD1 or CyaD2 in young nodules; *nsrA* is essential for secondary infection control. We discuss the structure of NsrA and the transmembrane signaling pathway by which it may control secondary infection.

RESULTS

***S. meliloti* CyaK senses nodule signal 1.** We previously observed, in crude extracts of mature nodules, the presence of a signal (referred to as signal 1) able to elicit reporter fusion (*smc02178-lacZ*) expression in free-living *S. meliloti* cultures, in a *cyaD1D2K*-dependent manner (8). After testing individual mutants, we found that CyaK was the cognate AC for nodule signal 1, since *cyaK* inactivation abolished signal 1-dependent expression of the *smc02178*-lacZ reporter fusion. In contrast, individual or combined inactivation of the *cyaD1* and *cyaD2* genes had no effect (Fig. 1), although

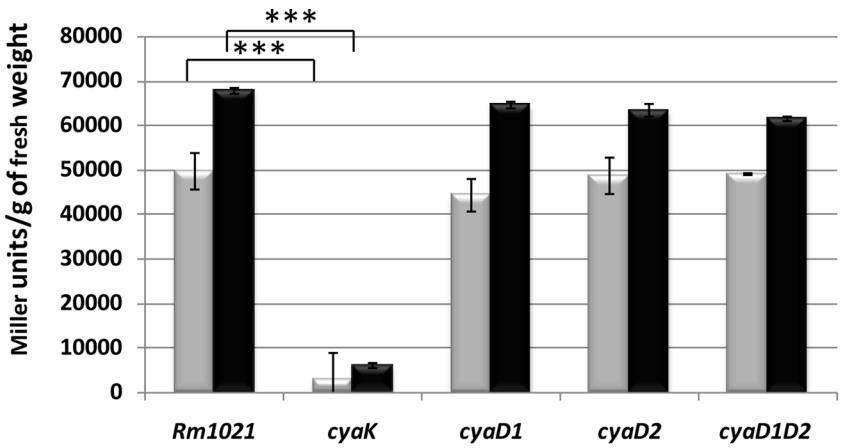

FIG 1 CyaK sensing of signal 1. *Ex planta* expression of the *smc02178-lacZ* fusion carried on the pGD2178 plasmid was assessed in the presence of shoot (gray bars) and 14-dpi nodule (black bars) extracts in *S. meliloti* wild-type (Rm1021), *cyaD1*, *cyaD2*, and *cyaK* genetic backgrounds. Activity was standardized per gram of shoot or nodule extract. ***, $P < 0.001$. Brackets indicate comparison with the reference sample.

the three AC genes were expressed at similar levels under free-living and symbiotic conditions (14). Therefore, CyaK is the cognate AC for nodule signal 1.

It is noteworthy that *cyaK* was also needed for the cell response to the shoot signal, which may indicate that the shoot signal is structurally close, if not identical, to nodule signal 1, although the possibility that CyaK responds to different signal molecules cannot be excluded. Nevertheless, for practical reasons, the shoot signal was used as a surrogate for nodule signal 1 in the experiments described below.

NsrA, a *S. meliloti* outer membrane protein, is required for signal 1 perception. We identified, upstream of *cyaK*, a long open reading frame (encoding 1,200 amino acids) corresponding to the *smb20775* (*nsrA*) gene (see https://iant.toulouse.inra.fr/bacteria/annotation/cgi/rhime.cgi). Based on the overlap of the stop codon of *nsrA* (underlined) with the start codon (bold) of *cyaK* (TG**ATG**), *nsrA* is likely cotranslated with *cyaK*.

In silico analysis of the NsrA protein revealed a complex structure (see Fig. S1 in the supplemental material). A cleavable signal peptide at the amino terminus of the protein was predicted by the SignalP program (15), indicating that the protein passes the inner membrane. Accordingly, the PSORTb v3.0 program (16) predicted an outer membrane location of the mature protein.

We compared the NsrA protein to proteins of known three-dimensional structure using PHYRE2 software (17). Because the NsrA protein is long, dividing its amino acid sequence into smaller pieces (e.g., amino acids 1 to 160, 160 to 620, and 500 to 1200) facilitated visualization of the structure. PHYRE2 analysis predicted with high confidence (>99%) two overlapping domains in the amino acid 24 to 160 region, namely, a domain (amino acids 24 to 105) corresponding to the RIN domain of the giant adhesion protein of *Marinomonas primoryensis* (18) and a FecR domain (amino acids 67 to 157). In the FecR protein of *Escherichia coli*, the periplasmic FecR domain achieves a signaling function by interacting with the signaling domain of the FecA outer membrane receptor, which is involved in iron dicitrate binding and transport. PHYRE2 also identified with 99.9% confidence, downstream of the FecR domain, five tetratricopeptide repeat (TPR) motifs (positions 238 to 611), which are presumably involved in protein-protein interactions. This prediction was confirmed using the dedicated TPRpred program (19) (Fig. S1B). Finally, PHYRE2 predicted that the carboxy-terminal region (amino acids 612 to 1200) of the NsrA protein consisted of a β-barrel. Accordingly, the PRED-TMBB interface (20) (http://bioinformatics.biol.uoa.gr/PRED-TMBB) predicted 22 β-strands found in porin-like outer membrane receptors such as FhuA and FecA, specifically using the posterior decoding algorithm (Fig. S2 and S3).

In order to assess the involvement of *nsrA* in signal 1 perception and transduction, we engineered a nonpolar deletion mutant of *nsrA*. Reverse transcription (RT)-PCR

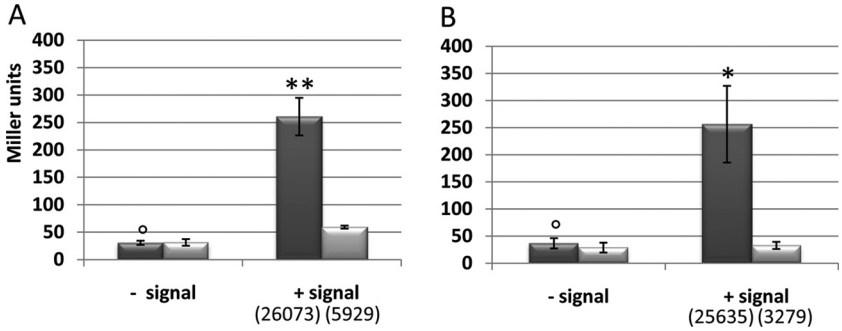

FIG 2 Need for *nsrA* for (shoot) signal 1 perception *ex planta*. (A) Expression of the *smc02178-lacZ* reporter fusion carried on the pGD2178 plasmid in Rm1021 (light gray bars) and *nsrA* mutant (dark gray bars) genetic backgrounds. (B) Expression of the *smb20495-lacZ* reporter fusion carried on the pGD20495 plasmid. *, $P < 0.05$; **, $P < 0.01$; °, reference sample. Mean specific activities (i.e., Miller units per gram of fresh weight) are indicated below the graph.

experiments confirmed the nonpolar character of the mutation and showed that the genes *nsrA* and *cyaK* were expressed independently of shoot signal 1 (Fig. S4). We found that the *nsrA* gene was absolutely required for shoot signal 1 perception *ex planta* by using two independent reporter fusions, *smc02178-lacZ* and *smb20495-lacZ* (12) (Fig. 2). Expression of the *smb20495-lacZ* reporter fusion was restored upon addition of exogenous cAMP (Fig. S5), indicating that the *nsrA* gene acts upstream of cAMP production by ACs, probably at the level of signal perception. We tentatively renamed the *smb20775* gene *nsrA* (nodule signal receptor A).

Overexpression of *nsrA* boosts the signal response *ex planta*. To elucidate the respective roles of *nsrA* and *cyaK* in signal 1 perception, we overexpressed the two genes from their native promoter, either individually or together, on pBBR1MCS-5 plasmid derivatives (Table 1). We found that the overexpression of *nsrA* alone

TABLE 1 Bacterial strains and plasmids used in this study

Strain or plasmid	Description[a]	Reference or source
DH5α	*E. coli fhuA2* Δ(*argF-lacZ*)*U169 phoA glnV44* ϕ80 Δ(*lacZ*)M15 *gyrA96 recA1 relA1 endA1 thi-1 hsdR17*	Bethesda Research Laboratories
1021 (Rm1021)	Derivative of *S. meliloti* strain SU47; Str^r	28
GMI11555	1021 Δ*cyaD2*::Gm Str^r Gen^r	8
GMI11556	1021 Δ*cyaK*::Gm Str^r Gen^r	8
GMI11557	1021 *cyaD1*::pVO155 Δ*cyaD2* Str^r Neo^r	8
GMI11558	1021 *cyaD1*::pVO155 Δ*cyaD2* Δ*cyaK*::Gm Str^r Neo^r Gen^r	8
GMI11561	1021 *cyaD1*::pVO155 Str^r Neo^r	8
GMI12049	1021 Δ*nsrA* Str^r	This work
GMI12050	1021(pGMI50331, pGD2178) Str^r Gen^r Tet^r	This work
GMI12051	1021(pGMI50332, pGD2178) Str^r Gen^r Tet^r	This work
GMI12052	1021(pGMI50333, pGD2178) Str^r Gen^r Tet^r	This work
GMI12053	1021 *cyaD1*::pVO155 Δ*cyaD2* Δ*cyaK* pGMI50331 pGD2178 Str^r Neo^r Gen^r Tet^r	This work
GMI12054	1021 *cyaD1*::pVO155 Δ*cyaD2* Δ*cyaK* pGMI50332 pGD2178 Str^r Neo^r Gen^r Tet^r	This work
GMI12055	1021 *cyaD1*::pVO155 Δ*cyaD2* Δ*cyaK* pGMI50333 pGD2178 Str^r Neo^r Gen^r Tet^r	This work
pJQ200-mp19	Suicide vector; Gen^r	25
pGEM-T	Cloning vector; Amp^r	Promega Corp.
pRK600	Helper conjugative plasmid, ColE1 replicon with RK2 transfer region; Chl^r	29
pGD926	pRK290 derivative containing promoterless *lacZ* gene; Tet^r	30
pXLGD4	*hemA-lacZ* reporter plasmid; Tet^r	31
pGD2178	pGD926 containing *smc02178* promoter region fused to *lacZ*; Tet^r	8
pGD20495	pGD926 containing *smb20495* promoter region fused to *lacZ*; Tet^r	12
pBBR1MCS-5	Cloning vector; Gen^r	32
pGMI50331	pBBR1MCS-5 derivative expressing *nsrA* and *cyaK*; Gen^r	This work
pGMI50332	pBBR1MCS-5 derivative expressing *cyaK*; Gen^r	This work
pGMI50333	pBBR1MCS-5 derivative expressing *nsrA*; Gen^r	This work
pGMI50334	pJQ200-mp19 derivative carrying deleted *nsrA* gene; Gen^r	This work

[a]Str^r, streptomycin resistance; Gen^r, gentamicin resistance; Neo^r, neomycin resistance; Chl^r, chloramphenicol resistance; Tet^r, tetracycline resistance; Amp^r, ampicillin resistance.

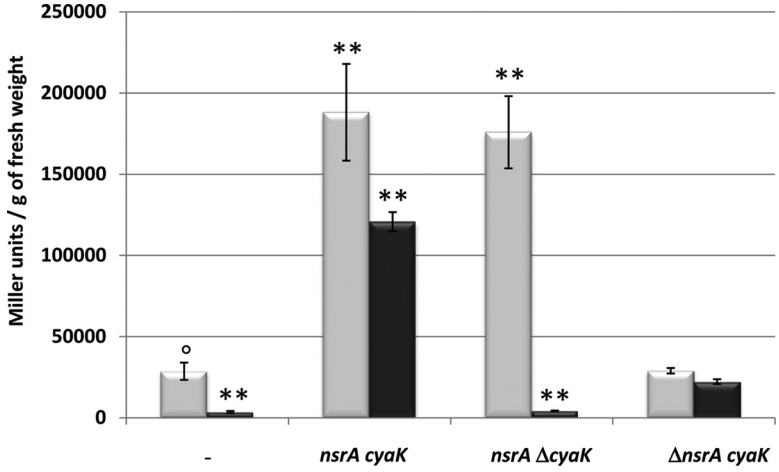

FIG 3 Plasmid-driven overexpression of *nsrA* increasing (shoot) signal 1 responses *ex planta*. Expression of the *smc02178-lacZ* fusion (pGD2178) was monitored in wild-type *S. meliloti* Rm1021 (gray bars) or the *cyaD1 cyaD2 cyaK* triple mutant (black bars). The relevant plasmid genotypes are indicated below the graph. **, $P < 0.01$; °, reference sample.

(pGMI50332) amplified the reporter gene response to shoot signal 1 by ~6-fold, indicating that NsrA is present in limiting amounts at the bacterial cell surface for signal 1 responses (Fig. 3), whereas overexpression of the *cyaK* gene alone (pGMI50333) had no effect (Fig. 3).

The *nsrA* gene is needed for secondary infection control. The nonpolar *nsrA* mutant of *S. meliloti* was inoculated on *Medicago sativa* (cv. Europe) seedlings, and expression of the *smc02178-lacZ* reporter gene fusion was assessed in mature (14-dpi) nodules. Eighty-two percent of *nsrA*-generated nodules remained white following β-galactosidase detection with 5-bromo-4-chloro-3-indolyl-β-D-galactopyranoside (X-Gal), whereas a *cyaK* mutant displayed only 37% completely white nodules (Fig. 4A; also see Fig. S6). Based on *smc02178-lacZ* expression, the *nsrA* mutant thus displayed a stronger phenotype than a single *cyaK* mutant or a *cyaD1 cyaD2 cyaK* mutant, close to that of a *clr* mutant (100% white nodules). The trend was the same with 7-dpi nodules, with the *nsrA* mutant more closely resembling a *cyaD1 cyaD2 cyaK* mutant than a *cyaK* mutant (Fig. S6).

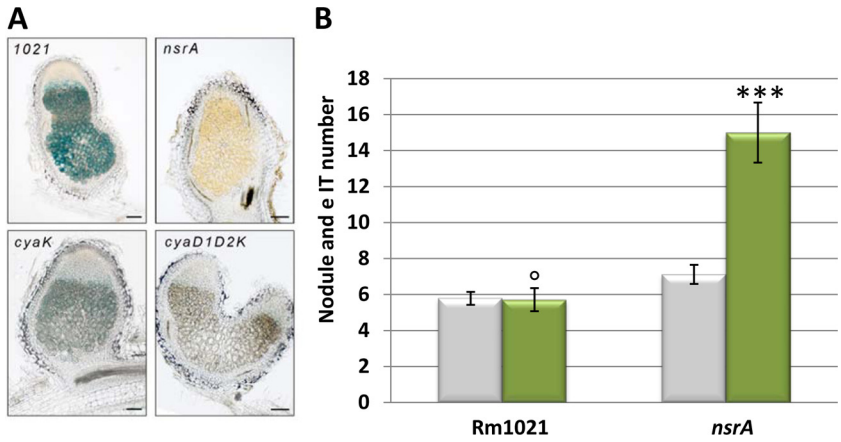

FIG 4 Phenotypes of the nonpolar *S. meliloti nsrA* mutant *in planta*. (A) *In situ smc02178-lacZ* (pGD2178) expression in *Medicago sativa* nodules (14 dpi) elicited by different *S. meliloti* strains. The predominant phenotype is shown (see the text and Fig. S6 for details). Scale bars = 100 μm. (B) Nodulation (gray bars) and hyperinfection (green bars) phenotypes of the *S. meliloti nsrA* mutant on *M. sativa* at 14 dpi. The pxLGD4 plasmid was introduced in the *S. meliloti nsrA* mutant to allow eIT visualization. ***, $P < 0.001$; °, reference sample.

We then tested the *nsrA* mutant for its secondary infection phenotype on *Medicago* roots at 14 dpi. We observed a marked hyperinfection phenotype for the *nsrA* mutant (Fig. 4B), similar to that described previously for a *cyaD1 cyaD2 cyaK* triple mutant or a *clr* mutant. In contrast, a *cyaK* mutant displayed only a weak hyperinfection phenotype (8). Nodule number (Fig. 4) and nitrogen fixation (as inferred from the pink color of nodules and the growth of plants) were unaffected by the *nsrA* mutation. Altogether, these findings indicate that the symbiotic phenotype of the *nsrA* mutant is stronger than that of a *cyaK* mutant and resembles that of a *cyaD1 cyaD2 cyaK* mutant.

DISCUSSION

Previously, we identified three ACs of the inner membrane in *S. meliloti* that play a role in signal perception and transduction during symbiosis. Here we describe an outer membrane sensor protein of *S. meliloti* that, together with the three ACs, allows plant signal perception by endosymbiotic bacteria and fine-tuning of the symbiotic interaction between *S. meliloti* and its host plant, *Medicago*.

Previous results indicated that all three cyclases, CyaD1, CyaD2, and CyaK, contribute to the control of secondary infection, since inactivation of the three cyclases was needed for a full hyperinfection phenotype (8). Furthermore, it was shown that CyaD1, CyaD2, and CyaK perform distinct and complementary functions in nodules. CyaK was the prominent AC in mature (14-dpi) nodules, as assessed by *smc01278* expression, whereas all three cyclases contributed to *smc01278* expression in younger (7-dpi) nodules (8). Here we provide additional support for this model by showing that signal 1, which is present in mature nodule extracts, is transduced by CyaK alone. Since CyaD1 and CyaD2 contribute to *smc02178* expression in young nodules (see Fig. S6 in the supplemental material), as well as to the control of secondary infection (8), we hypothesize the existence of a second signal (called signal 1′) triggering CyaD1 and/or CyaD2 activity in young nodules. In contrast to signal 1, however, we do not have direct biochemical evidence for the presence of signal 1′ in any biological material; its existence thus awaits confirmation. Furthermore, the assumption that the closely related CyaD1 and CyaD2 proteins sense the same signal 1′, as suggested here for simplicity, remains to be assessed.

In silico analysis allowed us to predict with good confidence the structure and topology of the NsrA protein. NsrA is made up of two moieties; the amino-terminal moiety of the protein (amino acids 24 to 600) is located in the periplasm, whereas the rest of the protein (amino acids 600 to 1200) is embedded in the outer membrane. The periplasmic moiety is composed of up to three domains, RIN, FecR, and TPR. The RIN and FecR domains, although overlapping, were both predicted with very high confidence by the PHYRE2 software (Fig. S1). The reality and biological significance, if any, of this overlap need to be clarified. Whether this portion of the NsrA protein can alternate between these two structural folds according to environmental conditions (e.g., the presence of a signal molecule) or whether the two domains are actually part of a single extended motif remains to be clarified. The second moiety of the protein is a β-barrel made up of 22 β-strands, as found in TonB-dependent transporters (TBDTs) such as FecA and FhuA from *E. coli* (Fig. S2). For unknown reasons, the β-barrel structure in NsrA was predicted only by the posterior prediction algorithm of the PRED-TMBB software (Fig. S2). This prediction was independently made with 100% confidence by the PHYRE2 program, however, and we consider it fully trustable.

We showed here that the *nsrA* gene was absolutely required for signal 1 perception *ex planta* (Fig. 2) and in mature nodules (Fig. 4A; also see Fig. S6 in the supplemental material). We also provided circumstantial evidence for NsrA perceiving a hypothetical signal 1′ in young nodules. Furthermore, *nsrA* was absolutely required for the negative control of secondary infection (Fig. 4B). Altogether, these findings suggest that NsrA is needed for signal perception by all three ACs (CyaD1, CyaD2, and CyaK) in nodules.

In the simplest working model (Fig. 5), two signals, namely, the outer membrane

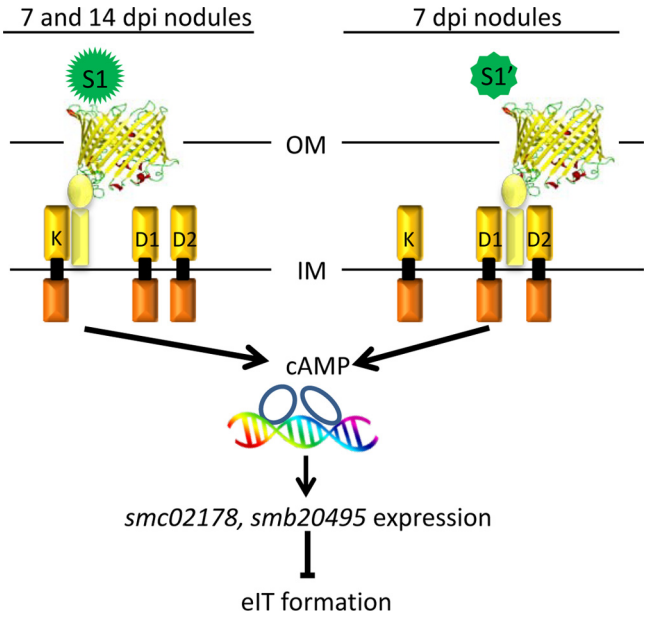

FIG 5 Working model for signal perception via NsrA, based on the predicted topology of NsrA (see the text for details). In young and mature nodules, signal 1 (S1) interacts with the β-barrel domain of NsrA (yellow). In our model, the periplasmic RIN/FECR (yellow rectangle) and/or TPR (yellow oval) domains of NsrA interact with the inhibitory CHASE2 domain (gold rectangle) of CyaK, releasing the activity of the cytoplasmic AC domain (orange rectangles). In the presence of cAMP, the Clr protein (blue ovals) activates target gene expression and inhibits eIT formation. In young nodules, a hypothetical signal 1′ (S1′) would bind NsrA and allow CyaD1 and/or CyaD2 activity. Together, both signal 1 and signal 1′ and the three ACs control secondary eIT formation. OM, outer membrane; IM, inner membrane.

receptor NsrA protein described here and the three ACs located in the inner membrane, together participate in the control of secondary root infection. Signal 1, which is the prominent signal in mature nodules, would be sensed and transduced by NsrA and CyaK, whereas the hypothetical signal 1′ would be sensed and transduced by NsrA and CyaD1 and/or CyaD2 in young nodules. We suggest here that the surface-exposed β-barrel of the NsrA protein (Fig. S3) acts as a receptor for both signal 1 and hypothetical signal 1′. Alternatively, signal 1 and signal 1′ may bind not NsrA itself but a yet-to-be identified cell surface protein that interacts with NsrA. Identification and further testing of signal 1 and signal 1′ should help discriminate between these two possibilities.

Transmembrane signaling (also called cell surface signaling or transenvelope signaling) addresses the mechanisms by which external signaling at the surface of the cell leads to gene expression in the cytoplasm. A paradigm for transmembrane signaling involves TBDTs, which are β-barrel proteins that are embedded in the outer membrane and serve both transport (e.g., of siderophores and vitamin B_{12}) and signaling functions. For example, FecA has two related functions in enteric bacteria; it imports ferric citrate into the cell and it also transcriptionally regulates the ferric citrate import operon via the inner membrane-associated FecR protein, which has anti-sigma factor activity (21, 22). Although NsrA shares with FecA and other TBDTs the carboxy-terminal β-barrel domain typically made up of 22 β-sheets (Fig. S2), the lack of the transport-related PLUG domain and TONB box domain in the periplasmic region of NsrA suggests that NsrA has no transport function and primarily plays a signaling role.

Furthermore, the signaling mechanisms for FecA and NsrA may be different. FecA interacts with the FecR periplasmic domain of the inner membrane-associated FecR protein via a short signaling domain (amino acid positions 1 to 80 in FecA) (22), whose nuclear magnetic resonance (NMR) structure has been solved (23). The signaling domain is missing in NsrA. Instead, a RIN/FecR domain is found in the periplasmic portion of NsrA, associated with a TPR domain. One or several of the periplasmic

domains of NsrA may interact with the periplasmic CHASE2 domain of the receptor-like ACs CyaK, CyaD1, and CyaD2, in the presence of the cognate plant signal (Fig. 5). This interaction would then trigger AC activity (i.e., cAMP synthesis from ATP) by relieving the negative impact of the CHASE2 domain on cytoplasmic AC activity, as demonstrated previously for CyaD1 (8).

Deciphering the role of the different domains of NsrA in signal perception and propagation may thus shed new light on transmembrane signaling in bacteria. It may also shed light on the mode of signal transduction of the CHASE2 domain, which is found in many signal-transducing proteins in bacteria, including ACs, histidine kinases, and serine/threonine kinases (7).

MATERIALS AND METHODS

Bacterial strains and culture conditions. Bacterial strains used in this study are listed in Table 1. Unless otherwise indicated, strains were grown at 28°C in Vincent minimal medium (VMM) (24) supplemented with mannitol (1%) and glutamate (0.1%) as carbon and nitrogen sources, respectively. The concentrations of antibiotics used for *S. meliloti* were 200 μg/ml for streptomycin and 10 μg/ml for tetracycline in both liquid and solid media. Gentamicin was used at 10 μg/ml and 30 μg/ml and neomycin at 50 μg/ml and 100 μg/ml in liquid and solid media, respectively. Primers used for DNA amplification are listed in Table S1 in the supplemental material.

Construction of the *S. meliloti* Rm1021 *nsrA* mutant (GMI12049). Deletion of the *nsrA* (*smb20775*) gene in Rm1021 was achieved in four steps. First, DNA fragments consisting of upstream and downstream regions of *nsrA* were generated by PCR using the 20775upL/20775upR and 20775downL/20775downR primer pairs, respectively (Table S1). PCR products were individually A-tailed with Taq polymerase and cloned into the pGEM-T plasmid (Table 1), giving rise to pGEm20775up and pGEM20775down plasmids. Second, the pGem20775down plasmid was digested with PstI and treated with the Klenow fragment of DNA polymerase I to generate blunt ends. After XbaI digestion, the purified *nsrA*-down DNA fragment was cloned into pGEM20775up digested with NcoI and blunt-ended using the Klenow enzyme. After ligation, the pGEM20775updown plasmid, in which the upstream and downstream parts of *nsrA* were cloned adjacently, was obtained. Third, the corresponding DNA fragment was recloned into the pJQ200mp19 suicide plasmid at the PstI and BamHI restriction sites to generate pGMI50334. Fourth, the pGMI50334 plasmid was introduced into *S. meliloti* by triparental mating using pRK600 as a helper plasmid, and the endogenous *nsrA* gene was marker exchanged using the *sacB* selection procedure (25).

Construction of the pGMI50331, pGMI50332, and pGMI50333 expression plasmids. To construct the pGMI50331 and pGMI50332 plasmids, we first amplified by PCR the DNA region encompassing the *nsrA* and *cyaK* genes from the wild-type Rm1021 strain and the *S. meliloti cyaK* mutant (GMI11556), respectively, using the psmb20775NdeI and smb20776SpeI primers (Table S1). To construct the pGMI50333 plasmid, we amplified by PCR the DNA region bracketed by the psmb20775NdeI and smb20776XbaI primers from the *S. meliloti nsrA* deletion mutant (GMI12049). The three PCR fragments (5,726 bp, 3,693 bp, and 2,965 bp) were then purified, digested with XbaI, and cloned into the pBBR1MCS-5 plasmid digested with XbaI and SmaI. The pGMI50331, pGMI50332, and pGMI50333 plasmids were transformed in the *E. coli* DH5α strain, verified by PCR and Sanger sequencing, and then introduced by triparental mating into the *S. meliloti* strain Rm1021 or the *cyaD1 cyaD2 cyaK* mutant (GMI11558).

Reverse transcription reactions. The three strains *of S. meliloti* (Rm1021, GMI11556, and GMI12049) (Table 1) were grown overnight at 28°C in VMM and diluted to an optical density at 600 nm (OD_{600}) of 0.12 in 20 ml of VMM. After overnight induction with a 10-fold dilution of a shoot extract (see below), 15 ml of the culture was filtered on Supor membrane disc filters (Pall) and stored at −80°C. RNA preparations were as described previously (26).

Reverse transcriptions were performed with 1 μg of RNA using the Transcriptor reverse transcriptase (Roche) and random hexamers as primers. cDNAs were subjected to PCR amplification (50 cycles) with DNA polymerase (Promega) and analyzed by SDS-PAGE. Controls included no-reverse-transcriptase samples and genomic DNA.

Shoot and nodule signal preparations. For plant extract preparation, *M. sativa* seedlings grown on Fahraeus medium in square plates were inoculated with *S. meliloti* Rm1021. Fourteen days postinoculation, nodules (approximately 150 to 200 mg [fresh weight]) were collected in Eppendorf tubes and immediately frozen in liquid nitrogen. Frozen nodules were crushed with a pestle, and the resulting material was resuspended in 1.5 ml of distilled water and centrifuged at 12,000 rpm for 8 min. The cleared supernatant was filtered through a 0.22-μm filter (Millipore) and stored at −80°C, if necessary, before assays.

Leaves (approximately 150 to 200 mg [fresh weight]) were ground cryogenically using glass beads (3-mm diameter) in a mixer mill, at a vibration frequency of 30 cycles/s. The resulting powder was resuspended in 800 μl of distilled water, and the debris was removed by centrifugation at 12,000 rpm for 8 min. The cleared supernatant was filtered and stored as described above.

***β*-Galactosidase assays and cytological techniques.** *S. meliloti* strains carrying the pGD2178 or pGD20495 plasmid (Fig. 1 to 3) were grown at 28°C in VMM. Overnight cultures were diluted to an OD_{600} of 0.1 in 1 ml of VMM supplemented with 100 μl of *Medicago* shoot signal (~19 mg total protein/100 μl) or nodule signal fresh extract (~10 mg protein/100 μl). The assays for β-galactosidase activity were

carried out using the protocol described by Miller (27). All experiments were performed at least in triplicate.

For *in planta* assays (Fig. 4A), *M. sativa* seedling plants were inoculated with *S. meliloti* strains (wild-type and mutant strains) carrying the pGD2178 plasmid (Table 1). Entire roots were collected 14 days after inoculation, fixed with 2% glutaraldehyde solution for 1.5 h under vacuum, rinsed three times in Z′ buffer (0.1 M potassium phosphate buffer [pH 7.4], 1 mM MgSO4, and 10 mM KCl), and stained overnight at 28°C, under vacuum, in Z′ buffer containing 0.08% X-Gal, 5 mM $K_3Fe(CN)_6$, and 5 mM $K_4Fe(CN)_6$. Nodules were harvested at 14 dpi, fixed with 2% glutaraldehyde in Z′ buffer, and then sliced into 80-μm-thick longitudinal sections using a vibrating-blade microtome (VT1000S; Leica, Heidelberg, Germany) before overnight staining at 28°C without vacuum. Nodule sections were observed under a light microscope. Hyperinfection phenotype determination (Fig. 4B) using pXLGD4 derivatives of the strains tested was conducted as described previously (8), with at least 14 plants per strain.

SUPPLEMENTAL MATERIAL

Supplemental material for this article may be found at https://doi.org/10.1128/JB.00019-18.

SUPPLEMENTAL FILE 1, PDF file, 1.4 MB.

ACKNOWLEDGMENTS

F.S. was supported in part by a postdoctoral AGREENSKILLS fellowship, L.Z. and C.F.T. were supported by CSC scholarships, and C.M.-D. was supported by a Ph.D. fellowship from the French Ministère de l'Enseignement supérieur et de la Recherche. This work was funded in part by the ANR RhizocAMP (ANR-10-BLAN-1719), the ANR AOI (ANR-15-CE20-0004-01), and the Pôle de Compétitivité Agri Sud Ouest Innovation. This work is part of the Laboratoire d'Excellence (LABEX) entitled TULIP (ANR-10-LABX-41).

REFERENCES

1. Masson-Boivin C, Giraud E, Perret X, Batut J. 2009. Establishing nitrogen-fixing symbiosis with legumes: how many rhizobium recipes? Trends Microbiol 17:458–466. https://doi.org/10.1016/j.tim.2009.07.004.
2. Masson-Boivin C. 2017. Symbiotic nitrogen fixation by rhizobia: the roots of a success story. Curr Opin Plant Biol 44:7–15. https://doi.org/10.1016/j.ceb.2016.11.002.
3. Suzaki T, Yoro E, Kawaguchi M. 2015. Leguminous plants: inventors of root nodules to accommodate symbiotic bacteria. Int Rev Cell Mol Biol 316:111–158. https://doi.org/10.1016/bs.ircmb.2015.01.004.
4. Long SR. 2016. SnapShot: signaling in symbiosis. Cell 167:582–582.e1. https://doi.org/10.1016/j.cell.2016.09.046.
5. Galibert F, Finan TM, Long SR, Puhler A, Abola P, Ampe F, Barloy-Hubler F, Barnett MJ, Becker A, Boistard P, Bothe G, Boutry M, Bowser L, Buhrmester J, Cadieu E, Capela D, Chain P, Cowie A, Davis RW, Dreano S, Federspiel NA, Fisher RF, Gloux S, Godrie T, Goffeau A, Golding B, Gouzy J, Gurjal M, Hernandez-Lucas I, Hong A, Huizar L, Hyman RW, Jones T, Kahn D, Kahn ML, Kalman S, Keating DH, Kiss E, Komp C, Lalaure V, Masuy D, Palm C, Peck MC, Pohl TM, Portetelle D, Purnelle B, Ramsperger U, Surzycki R, Thebault P, Vandenbol M, Vorholter FJ, Weidner S, Wells DH, Wong K, Yeh KC, Batut J. 2001. The composite genome of the legume symbiont *Sinorhizobium meliloti*. Science 293:668–672. https://doi.org/10.1126/science.1060966.
6. Capela D, Barloy-Hubler F, Gouzy J, Bothe G, Ampe F, Batut J, Boistard P, Becker A, Boutry M, Cadieu E, Dreano S, Gloux S, Godrie T, Goffeau A, Kahn D, Kiss E, Lelaure V, Masuy D, Pohl T, Portetelle D, Puhler A, Purnelle B, Ramsperger U, Renard C, Thebault P, Vandenbol M, Weidner S, Galibert F. 2001. Analysis of the chromosome sequence of the legume symbiont *Sinorhizobium meliloti* strain 1021. Proc Natl Acad Sci U S A 98:9877–9882. https://doi.org/10.1073/pnas.161294398.
7. Zhulin IB, Nikolskaya AN, Galperin MY. 2003. Common extracellular sensory domains in transmembrane receptors for diverse signal transduction pathways in *Bacteria* and *Archaea*. J Bacteriol 185:285–294. https://doi.org/10.1128/JB.185.1.285-294.2003.
8. Tian CF, Garnerone AM, Mathieu-Demaziere C, Masson-Boivin C, Batut J. 2012. Plant-activated bacterial receptor adenylate cyclases modulate epidermal infection in the *Sinorhizobium meliloti-Medicago* symbiosis. Proc Natl Acad Sci U S A 109:6751–6756. https://doi.org/10.1073/pnas.1120260109.
9. Murray JD. 2011. Invasion by invitation: rhizobial infection in legumes. Mol Plant Microbe Interact 24:631–639. https://doi.org/10.1094/MPMI-08-10-0181.
10. Miri M, Janakirama P, Held M, Ross L, Szczyglowski K. 2016. Into the root: how cytokinin controls rhizobial infection. Trends Plant Sci 21:178–186. https://doi.org/10.1016/j.tplants.2015.09.003.
11. Vasse J, Debilly F, Truchet G. 1993. Abortion and infection during the *Rhizobium meliloti*-alfalfa symbiotic interaction is accompanied by a hypersensitive reaction. Plant J 4:555–566. https://doi.org/10.1046/j.1365-313X.1993.04030555.x.
12. Zou L, Gastebois A, Mathieu-Demaziere C, Sorroche F, Masson-Boivin C, Batut J, Garnerone AM. 2017. Transcriptomic insight in the control of legume root secondary infection by the *Sinorhizobium meliloti* transcriptional regulator Clr. Front Microbiol 8:1236. https://doi.org/10.3389/fmicb.2017.01236.
13. Krol E, Klaner C, Gnau P, Kaever V, Essen LO, Becker A. 2016. Cyclic mononucleotide- and Clr-dependent gene regulation in *Sinorhizobium meliloti*. Microbiology 162:1840–1856. https://doi.org/10.1099/mic.0.000356.
14. Capela D, Filipe C, Bobik C, Batut J, Bruand C. 2006. *Sinorhizobium meliloti* differentiation during symbiosis with alfalfa: a transcriptomic dissection. Mol Plant Microbe Interact 19:363–372. https://doi.org/10.1094/MPMI-19-0363.
15. Petersen TN, Brunak S, von Heijne G, Nielsen H. 2011. SignalP 4.0: discriminating signal peptides from transmembrane regions. Nat Methods 8:785–786. https://doi.org/10.1038/nmeth.1701.
16. Yu NY, Wagner JR, Laird MR, Melli G, Rey S, Lo R, Dao P, Sahinalp SC, Ester M, Foster LJ, Brinkman FSL. 2010. PSORTb 3.0: improved protein subcellular localization prediction with refined localization subcategories and predictive capabilities for all prokaryotes. Bioinformatics 26:1608–1615. https://doi.org/10.1093/bioinformatics/btq249.
17. Kelley LA, Mezulis S, Yates CM, Wass MN, Sternberg MJE. 2015. The Phyre2 web portal for protein modeling, prediction and analysis. Nat Protoc 10:845–858. https://doi.org/10.1038/nprot.2015.053.
18. Guo S, Stevens CA, Vance TDR, Olijve LLC, Graham LA, Campbell RL, Yazdi SR, Escobedo C, Bar-Dolev M, Yashunsky V, Braslavsky I, Langelaan DN, Smith SP, Allingham JS, Voets IK, Davies PL. 2017. Structure of a 1.5-MDa adhesin that binds its Antarctic bacterium to diatoms and ice. Sci Adv 3:e1701440. https://doi.org/10.1126/sciadv.1701440.
19. Karpenahalli MR, Lupas AN, Soding J. 2007. TPRpred: a tool for prediction of TPR-, PPR- and SELI-like repeats from protein sequences. BMC Bioinformatics 8:2. https://doi.org/10.1186/1471-2105-8-2.

20. Bagos PG, Liakopoulos TD, Spyropoulos IC, Hamodrakas SJ. 2004. PRED-TMBB: a web server for predicting the topology of β-barrel outer membrane proteins. Nucleic Acids Res 32:W400–W404. https://doi.org/10.1093/nar/gkh417.
21. Braun V, Mahren S, Ogierman M. 2003. Regulation of the FecI-type ECF sigma factor by transmembrane signalling. Curr Opin Microbiol 6:173–180. https://doi.org/10.1016/S1369-5274(03)00022-5.
22. Noinaj N, Guillier M, Barnard TJ, Buchanan SK. 2010. TonB-dependent transporters: regulation, structure, and function. Annu Rev Microbiol 64:43–60. https://doi.org/10.1146/annurev.micro.112408.134247.
23. Ferguson AD, Amezcua CA, Halabi NM, Chelliah Y, Rosen MK, Ranganathan R, Deisenhofer J. 2007. Signal transduction pathway of TonB-dependent transporters. Proc Natl Acad Sci U S A 104:513–518. https://doi.org/10.1073/pnas.0609887104.
24. Becker A, Berges H, Krol E, Bruand C, Ruberg S, Capela D, Lauber E, Meilhoc E, Ampe F, de Bruijn FJ, Fourment J, Francez-Charlot A, Kahn D, Kuster H, Liebe C, Puhler A, Weidner S, Batut J. 2004. Global changes in gene expression in *Sinorhizobium meliloti* 1021 under microoxic and symbiotic conditions. Mol Plant Microbe Interact 17:292–303. https://doi.org/10.1094/MPMI.2004.17.3.292.
25. Quandt J, Hynes MF. 1993. Versatile suicide vectors which allow direct selection for gene replacement in Gram-negative bacteria. Gene 127:15–21. https://doi.org/10.1016/0378-1119(93)90611-6.
26. Bobik C, Meilhoc E, Batut J. 2006. FixJ: a major regulator of the oxygen limitation response and late symbiotic functions of *Sinorhizobium meliloti*. J Bacteriol 188:4890–4902. https://doi.org/10.1128/JB.00251-06.
27. Miller G. 1972. Experiments in molecular genetics. Cold Spring Harbor Laboratory Press, Cold Spring Harbor, NY.
28. Meade HM, Long SR, Ruvkun GB, Brown SE, Ausubel FM. 1982. Physical and genetic characterization of symbiotic and auxotrophic mutants of *Rhizobium meliloti* induced by transposon Tn*5* mutagenesis. J Bacteriol 149:114–122.
29. Finan TM, Kunkel B, Devos GF, Signer ER. 1986. Second symbiotic megaplasmid in *Rhizobium meliloti* carrying exopolysaccharide and thiamine synthesis genes. J Bacteriol 167:66–72. https://doi.org/10.1128/jb.167.1.66-72.1986.
30. Ditta G, Schmidhauser T, Yakobson E, Lu P, Liang XW, Finlay DR, Guiney D, Helinski DR. 1985. Plasmids related to the broad host-range vector, pRK290, useful for gene cloning and for monitoring gene expression. Plasmid 13:149–153. https://doi.org/10.1016/0147-619X(85)90068-X.
31. Leong SA, Williams PH, Ditta GS. 1985. Analysis of the 5′ regulatory region of the gene for δ-aminolevulinic-acid synthase of *Rhizobium meliloti*. Nucleic Acids Res 13:5965–5976. https://doi.org/10.1093/nar/13.16.5965.
32. Kovach ME, Phillips RW, Elzer PH, Roop RM, Peterson KM. 1994. pBBR1MCS: a broad host-range cloning vector. Biotechniques 16:800–802.